Chapter 11

Acrylated-Epoxidized Soybean Oil-Based Polymers and Their Use in the Generation of Electrically Conductive Polymer Composites

Susana Hernández López and
Enrique Vigueras Santiago

Additional information is available at the end of the chapter

http://dx.doi.org/10.5772/52992

1. Introduction

1.1. Electrical properties on polymer compounds with carbon black making emphasis in the polymer matrix for controlling them

Polymer composites with electrical properties modified by the amount of conductive filler particles emerge at a half of the XX Century. This type of materials are conformed by two components, the first is usually majority and continuous component known as matrix and the second is the minority and discontinuous frequently named conductive filler. Both, matrix and filler could be constituted by one or many different materials. For example, the matrix could be only one polymer or it may well be constituted by a polymer blend, the same way the conductive component. The polymer composites are characterized for being multiphase materials in which is possible to distinguish the two phases: polymer and conductive filler. The own properties of these composites are determined by the synergic coupling between properties of the matrix and the conductive particles, this means the electrical conductivity on these composites and in turn on their practical applications are determined by the chosen polymer matrix-conductive filler couple.

Modification of the electrical properties in polymer composites based on carbon black (CB) particles could reach until 10^{11} orders of magnitude. This characteristic has allowed designing materials with applications for electrostatic protection and electromagnetic shields. It is well known that electrical properties are modified by external factors making them useful for applications as vapor, gases, toxic or inert substances sensors as well as detectors of temper-

ature and external mechanical strengths. For this reason from the 70´s the massive develop of polymer compounds plus conductive particles becomes important [1] and from the beginning it has been used all type of oleo-polymers and conductive particles being of major interest the carbon particles and nanoparticles. These carbonaceous particles allow obtaining polymer composites highly conductive, at great scale, at low cost, with the inherent polymer properties as lightness, processability into different shapes, sometimes reinforced in mechanical and thermal properties. The CB particles have very good conductivity thanks to a series of structural characteristics as the graphitic composition, the structure of the fundamental aggregate that could be low, middle or high, being a high structure [1] the required in order to render lower critical volume or weight percent (wt%) fractions. The particle surface is another important characteristic to take in account for having a good dispersion into the polymer. Some CB surfaces are oxidized and contain many functional groups as hydroxyls, carbonyls, esters, etc [1] which facilitate the interaction with the polymer matrix having a very good dispersion in it. Those and other characteristics as their easy synthesis at great scale make them the most studied conductive particles for preparing conductive polymer composites.

If the difference in the electrical conductivity between conductive particles and the matrix is at least six orders of magnitude then the electrical conductivity of polymer compounds in terms of the conductive particles load could be explained very well by the percolation concept [2]. According to this concept the electrical conductivity is achieved when the conductive particles reach a critical fraction which is the smallest amount of particles required to build a conductive network. This is established by the relationship 1.

$$\sigma(X) \approx (X - X_c)^{\beta} \tag{1}$$

X represents the volumetric fraction of the conductive filler, X_c the amount of conductive particles in the percolation threshold and is a critical exponent. The critical parameters Xc and β determine the transition from the dielectric to the conductive state in those polymer composites. This make an important difference in the electrical properties respect to the conventional materials in which is possible to determine the type of material according to the order of magnitude in its electrical conductivity. In composite materials the electrical conductivity is achieved when a volume or weight filler fraction is reached and it is characterized because the particles are in electric contact building conductive paths. In this conductive network the electrical interconnection is favored when the transit of electrons is allowed from one particle to another; transitions which are governed by the mechanical quantum laws [3]. The percolation model given by equation 1 fits very well to the experimental results allowing to explain the mechanism for which these composites could be considered as intelligent materials, useful for the detection of temperature gradients, pressure, displacement, solvents, gases, etc. For all those reasons the percolation model has been accepted as the well way to explain the electric conduction in terms of conductive particles fraction. However it has the important disadvantage to no predict the percolation threshold for a specific polymer-conductive particles couple.

http://dx.doi.org/10.5772/52992

Such disadvantage emerges from the fact that it only considers the particles interconnection probability without taking in account the polymer matrix nature and the possible interactions between particles and polymer.

The critical fraction is also associated with the potential applications of the polymer composite. In polymer composites with high critical fraction the mechanical properties could be influenced due the secondary forces between polymer chains are modified by the presence o a high fraction of particles and as a consequence the mechanical properties of the composite could detriment. On another hand in solvent sensing applications it has been demonstrate that as lower conductive particles fraction the sensibility to the detection is considerably increased due to the best interaction area between the polymer and the solvent, vapor or gas [4]. This is the reason for which one of the goals in the preparation of conductive composites is to diminish the critical fraction of conductive particles in conductive polymer composites. However there is not a generalized rule which allow predicting it considering both the polymer and the conductive particles properties. It is known that properties of the matrix polymer as density, viscosity at molten state, dielectric constant and those of the conductive particles as oxidative surface, size, shape and structure, have an important influence in the electrical composite properties in junction with the preparation method [1, 5-17]. The conditions in preparation method are especially important to achieve a homogeneous disaggregation and dispersion of the conductive particles and in turn to reach the electrical properties at a low fraction of conductive particles. A preferential and controlled distribution of those particles contributes to build conductive networks at a low critical fraction and it also guarantees a better reproducibility. Some strategies to obtain a preferential distribution have used polymer matrix derived from two or more immiscible polymers (blends) [10] in which the particles are in the interphase; the *in situ* synthesis using the emulsion polymerization [11] in which particles prefer to surround the polymer matrix nanoparticles. The polymer matrix viscosity [8] is very important to take in account for the conductive particles dispersion. In a high viscose polymer are required high shear forces in order to produce a disaggregation of the particles but also it could produce a breaking of the CB particles structure. This last effect is not convenient due are necessary more particles to interconnect them and form the conductivity network, increasing the critical fraction. Usually the strength distribution is not uniform, not a good dispersion is achieved and the conductivity is not reached a low fraction of conductive particles. In summary the polymers with low viscosity tend to reach the percolation threshold at a lower critical fraction in comparison with polymers highly viscose. The weight molecular mass [12] also influences the process of conductive particles distribution and is directly associated with the viscosity. In according with the latest discussion, as higher the molecular weight the polymer has a higher viscosity and viceverse, in such a way that conductive particles have less problems to disperse in a low molecular weight matrix. The polymer morphology [13] determines in some way the preparation process and the critical fraction of the conductive particles in the percolation threshold. It has been well established that particles tend to disperse uniformly in the amorphous region. As a consequence in semicrystalline matrixes is possible to have a preferential distribution of the conductive particles in the

amorphous and interphases zones diminishing the critical fraction. In other cases the polarity of the polymer matrix has taken in account for dispersing CB particles and there are many opinions respect to its influence on the critical fraction [9, 14,15]. It has been mentioned that a major polarity the critical fraction increases [9]. However other authors claim [14, 15] that a major polarity the particles dispersion is better due to the interactions between the groups on the surface of the CB particles and those on or pending on the polymer chain favoring their dispersion. Recently in a systematic study [16] has been demonstrated that critical fraction of CB particles included in some polystyrene-based polymers with different dielectric constant, tend to diminish as the polarity (dielectric constant) of the polymer matrix increases.

In other recently studies, has been evaluated that polymer derivate from vegetable oils as the soybean and linseed oil and some derivates have a very good compatibility not only with some natural fillers as fibers, henequen, cellulose, bamboo, etc, but also with CB particles and carbon nanotubes producing composites with a huge gamma of mechanical and thermal properties, similar to those offered for oleo-polymers, with a great potential to use them as engineering applications. Much less research has been focus to the electrical properties however those studies shown that critical fraction in composites based on acrylated-epoxidized soybean oil and epoxidized linseed oil with CB are much lower (lower than 4 wt% CB) than those exhibited by common oleo-polymers (usually higher than 8 wt % CB) [17]. This fact has been explained in terms of the functional groups of the polymer matrixes and on the ability to crosslink drawing paths in which the CB particles are favorable dispersed. In order to understand this phenomena, the next section will be devoted to describe the structure, characteristics and uses of vegetable oils, specifically focus to one derivate of soybean oil, the acrylated-epoxidized soybean oil (AESO) a derivate well studied as monomer and comonomer in the preparation of conductive composites with different CB particles.

1.2. Acrylated-epoxidized soybean oil: Some relevant advances and achievements

Polymeric materials prepared from renewable natural resources have become increasingly important because of their low cost, ready availability, and potential biodegradability. Vegetable oils represent one of the cheapest and most abundant biological feedstocks available in all around the world in large quantities, and their use as starting materials offers numerous advantages, such as low toxicity, biocompatibility, inherent biodegradability as well as certain excellent frictional properties e.g. good lubricity, low volatility, high viscosity index, solvency for lubricant additives, and easy miscibility with other fluids, and more recently in useful polymers and polymer composites [18-21].

In addition to their application in medicine, cosmetics, surfactants, nutrition, food industry, lubricants and as an alternative fuel for diesel, natural oils also have been used quite extensively to produce coatings, inks [22] plasticizers, lubricants, and agrochemical [23]. Structurally vegetable oils are predominantly constituted of triglyceride molecules. Triglycerides in turn are constituted of three fatty acids joined at a glycerol central structure. Most common oils contain fatty acids that vary from 14 to 22 carbons in length, with 0 to 3 double bonds per fatty

http://dx.doi.org/10.5772/52992

acid. Because of the many different fatty acids present, these oils are composed of many different types of triglycerides with numerous levels of unsaturation. A high degree of multiple unsaturations (-C=C-) in the fatty acid (FA) chain of many vegetable oils causes poor thermal and oxidative stability and confines their use as lubricants to a modest range of temperature [24]. Although they possess double bonds, which could be used as reactive sites, they are of low reactivity and cross-linked polymers could be produced under a specific and limited reaction conditions [25-29]. Usually as triglycerides are made up of aliphatic chains, the produced materials lack of the necessary rigidity and strength required for some applications. To reach a higher level of molecular weight and crosslink density is necessary to copolymerize [30-34] or to incorporate chemical functionalities [35] easily to polymerize and that are known to improve the mechanical properties of the polymer networks. The double bonds are usually used to functionalize the triglyceride with polymerizable chemical groups, for example to convert the unsaturation to epoxy group is the most common reaction. There are a lot of published studies devoted to establish [36-40], control [41, 42] and scale [43] many different reaction conditions for partial [44-46] or complete epoxidization of the trygliceride´s double bonds. By themselves the epoxidized oils are polymerizable under temperature [47-49] ultraviolet radiation [50-53], or by opening epoxy ring reaction. However is well know that the diamines [54, 55], anhydrides [56, 57], dicarboxylic acids [56], dioles [58, 59] are also used for curing epoxidized oils rendering cured resins with a gamma of properties controlled by the stoichiometry, the structure of the crosslinker and the cure degree.

Epoxidation in general is a commercially important reaction due to the high reactivity of that functional group that makes it to be readily transformed into other important functional and polymerizable groups. The most studied and important polymerizable groups are hydroxyl by complete or partial ring opening reaction of epoxy group [60] making the triglyceride capable of reaction via addition polymerization for producing polyurethanes [61-63] or hydroxylated polyesters for example with maleic anhydride which could further being cured by free radical reaction. Another important functional group is the acrylate inserted by reaction of epoxidized vegetable oils with acrylic acid [18, 64]. This last modification provides monomers which can then be blended with reactive diluents and cured by free radical polymerization. There are natural oils comprise fatty acids with these types of functionalities as the vernonia oil which contain epoxy groups and castor oil that comprise hydroxyl groups.

Soybean oil is an exemplar model of how the natural oils can be used for producing polymer and polymer composites useful in some applications. About 80% of the soybean oil produced each year is used for human food. Another 6% is exploiting for animal feed, while the remainder (14%) has nonfood uses (soap, fatty acids, lubricants, coatings, etc.). Structurally (Figure 1), soybean oil usually contains in average 11% palmitic, 4% stearic, 23% oleic, 54% linoleic and 8% linolenic acids. Palmitic acid contains 16 length carbons and no unsaturations, the remanent acids are all of them are 18 length carbons and are unsaturated acids: oleic (1 double bond), linoleic (2 unsaturations) and linolenic (3 double bonds). Soybean oil contain in average 4.5 double bonds which are thermally polymerizable under the special conditions above mentioned.

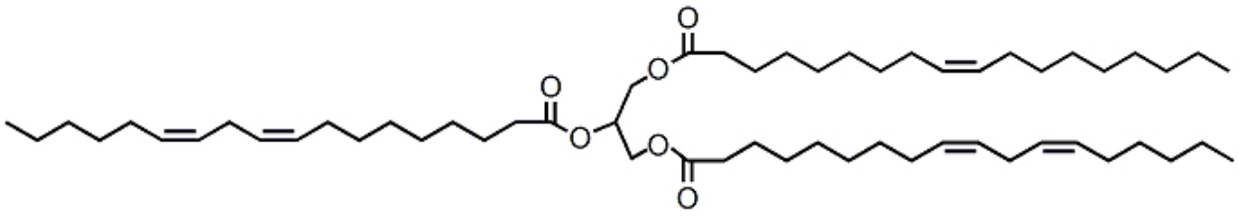

Figure 1. Representative structure of SBO showing three 18 carbon-length chains with 1 and two double bonds

For example, cationic polymerization of the soybean oil with divinylbenzene comonomer initiated by boron trifluoride diethyl etherate produces crosslinked polymers with properties from the rubbers (soft) to the thermosets (rigid) [34, 65]. These properties are dependent on the stoiquiometry of both comonomers. Some others copolymers prepared also by cationic polymerization [66] showed shape-memory effect which refers to the ability to remember a specific shape after deformation. Polymerized soybean oils have already been employed in printing inks and paints and much effort has been devoted to converting soybean oils into solid polymeric materials which now usually possess viable mechanical properties and thus may be useful as structural materials in a variety of specific applications [67]. In this context, one of the most important derivate is the epoxidized soybean oil (ESO). The epoxidized soybean oil is widely used as plasticizer instead of phtalates in the plastic industry to increase flexibility, stability and processability in PVC products. For this application the higher the epoxy degree more efficient is the stabilizer ability [41] to heat and UV-radiation. It was also studied as potential source of high-temperature lubricant [24]. It shows a low thermal and oxidative deteriorate compared with raw soybean oil and other oils due to the absence of allyl hydrogens which are the responsible of those unwanted process. Crosslinked polyesters were prepared by curing ESO with different dicarboxylic acid anhydrides [56]. The mechanical and thermal properties were evaluated and they were dependent on the type of anhydride, the type and wt% of catalyst and on the ratio ESO/anhydride. A broad range of glass transition temperatures, T_g´s, from -5 to 75°C were shown and flexural modulus from 520 to 980 MPa. Another example of ESO cured with different acid anhydrides [57] in presence of tertiary amines as initiators. The dynamical mechanical properties were studied in terms of the type of anhydride, initiator and epoxidation level. Composites based on ESO resin and chicken feathers fibers (CFFs) were studied as potential applications in electronic devices such as printed circuits and boards (PCBs) [68]. Equipment based on PCBs requires high electrical resistance, relatively low electric constant and loss. Properties were compared with those of the prepared composites using the standard epoxy resin for PCBs and CFFs as reinforcement. The resistivity of CFFs composites was two to four orders of magnitude higher than E-glass fiber composites indicating that CFFs have better insulating effect. The CFF composite can be potentially used as PCBs industry. In other study ceramer coatings based on ESO were prepared using three sol-gel titanium (IV) and zirconium precursors and several coating properties were evaluated, exhibiting excellent flexibility and hardness. Ceramer coatings (inorganic/organic hybrid materials) have potential applications in protecting optical and electronic devices. In this study the properties of ELO as low volatile organic content, low price and viscosity were taken in advantage in order to prepare the mentioned ceramers [69].

http://dx.doi.org/10.5772/52992

Another important derivate of soybean oil (Figure 2), in which this chapter will be devoted, is the acrylated-epoxidized soybean oil (AESO), produced in two steps from soybean oil. The first one is the epoxidation of soybean oil by any described method. After, this epoxy intermediate is reacted with acrylic acid [21, 64] in presence of an acid as catalyst, being the level of acrylatation very important for the mechanical properties as studied in [70]. T_g increases linearly with the number of acrylates per triglyceride from -50 to 92°C for 0.6 to 5.8 acrylates per triglyceride and it is possible to obtain soft and rigid polymers as the level of acrylatation increases.

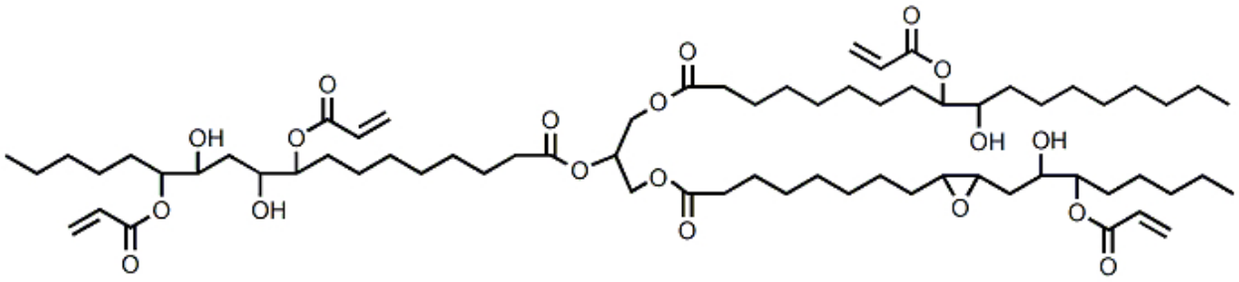

Figure 2. Representative structure for AESO

This molecule is interesting due the possibility of use the double bonds from acrylate functional group in order to polymerize/copolymerize easily via free radicals reaction under several initiator systems as thermal initiator decomposition, photoinitiators and UV or visible radiation, and high energy radiations as gamma rays. However, pure AESO polymer (polyAESO) does not display important mechanical properties by itself. It looks like an amorphous crosslinked rubber without possibility of processing in useful shapes. However these properties were taken in advantage for modify the mechanical and tribological properties of goat leather [71]. Elastic modulus, tensile deformation, friction and wear were evaluated for goat leather before and after to graft AESO monomer by each and both faces of the leather. The grafting was made by free radicals using a photonitiator and ultraviolet light as initiator system [72]. Those properties were dependent on the irradiation dosages (360, 720 and 2700 J/m^2) being the changes more evident at higher dosages and on the grafted face (inner or outer). In general friction and tensile deformation decreased (17% and 39%) respect to ungrafted leather whereas elastic modulus and wear decreasing as the dosage increased (19% and 39%, respectively).

However for engineering applications polyAESO do not have enough mechanical properties. An attempt to improve the mechanical properties of polyASEA was made using gamma radiation as initiator system [73]. In this work AESO was successfully polymerized and the polyASEA was obtained in one transparent and homogeneous piece depending on the used mold for polymerization. That piece could be cut in different shapes. Its properties as friction and scratch were evaluated respect to the dosage irradiation which was directly related to the crosslink degree. Some probes were made for preparing composites with carbon black under the same conditions, not rendering the same successfully results. In this case those composites were obtained as an unshaped mass without the possibility to processing them into specific shapes.

It is because AESO use to be copolymerized with other vinyl comonomers. The most used is the styrene comonomer which imparts stiffness and as the same time is useful as diluent in order to reduce the viscosity which is of great help when some filler is used for preparing polymer composites. In this context, a lot of interesting works have been published. These resins have proven to be comparable to commercial, oleo-based thermosetting resins. Also, AESO has been combined with several natural fibers [74] and other fillers as glass or carbon fibers and clays in order to produce new economical composites and very useful in many fields like agricultural, automotive, infrastructures, housing, and construction. Some examples are cited. Network blends of polyurethane network films were prepared using polyester urethane acrylate (PUA) having terminal double-bond functional groups and acrylated epoxidized soybean oil by a simultaneous thermal polymerization process. The weight ratios of PUA/AESO affected the thermal and mechanical properties; with an increase in AESO content the glass-transition temperature of the networks decreased from 40 to -4.8 °C, tensile strength increased from 1.2 to 9.8 MPa, and elongation at break decreased from 470 to 70% [75]. Copolymers of AESO and styrene mixed with butyrated kraft lignin as compatibilizing agent for natural fiber reinforced thermoset composites were prepared and evaluated [76]. An improvement of adhesion of the resin to the fibers was achieved and the flexural strength increased 40% for a 5 wt% butyrate lignin. The effect of different lignin concentrations on the mechanical properties of composite made of flax and wheat straw fibers, was investigated. The ultimate goal was a lignin-based, soluble additive that gives rise to a very strong resin-natural fiber interface. For construction structural panels and unit beams were manufactured from AESO and natural fibers (flax, cellulose, pulp, recycled paper and chicken feathers) as natural fiber reinforcements (20-55 wt%), E-glass fiber and closed cell structural foam achieve good mechanical strength. The goal of this work [77] was to develop monolithic structural panels that would be suitable for use as the (load-bearing) roof, floors or walls of a home. It was compared the mechanical properties. In summary, the results show that the recycled paper beam with chicken feathers and the recycled paper beam with corrugated cardboard have flexural rigidities for a commercial wood product. The beam with some E-glass is a stiff as stiff as other three of the wood commercial references. All composites beams are stronger than the woods references. In conclusion the composite beams made for recycled paper have strengths and stiffness that make them suitable for use in structural applications where wood members would normally used. Other important works are they where AESO was copolymerized with styrene in presence of cellulose fibers or corrugated cardboard boxes [78] in order to manufacture composites structures useful for residential roof construction, rendering successfully results according to the evaluated mechanical properties.

AESO/Styrene in a 65/35 wt ratio and 3 wt% of SWNT composites were prepared [79] by sonication procedure in order to study the mechanical properties. It was found that the addition of NTC results in an increasing of the flexural modulus about in a 44% and the yield strength in 9% as well as the T_g in 8%. In other work AESO/styrene (65/35 wt ratio) also has been reinforced with impure multi walled carbon nanotubes (containing 60-70% of carbon soot) with an aspect ratio of 33.3 [80]. Impure MWNT were added in 1, 3 and 5 wt% to the monomers mix and the dispersion conditions were evaluated until obtain a stable dispersion. Mixes were polymerized via free radicals using tert-butyl peroxy benzoate as initiator and

http://dx.doi.org/10.5772/52992

after their mechanical properties were analyzed. Modulus was increased respect to the same resin composition without MWNT in a 30% for samples having 1wt% MWNT. In both cases electrical properties were not evaluated.

However, electrical properties of polymer composites based on AESO and AESO copolymers with carbon black were studied [17]. As mentioned before, crosslinked polyAESO is not adequate to processes the respective composites into convenient shapes for evaluate electrical and other properties. Nevertheless, something that was very interesting is that the percolation concentration for this type of composite was very low (4.1 wt% CB) in comparison with those obtained with the traditional oleo-polymers based composites with carbon black as polystyrene (15 - 9.4) [16, 81], low density polyethylene (17%), polybutyl methacrylate (14%) [17], etc. This behavior is one evidence that polymer matrix in conjunction with the carbon black characteristics, is another parameter that has a very important influence in reach the percolation threshold at low critical fraction of conductive particles. A possible explanation is that AESO helps to low the concentration percolation due to CB particles disperse very well thanks to the presence of the carbonyl groups on the acrylic functional groups that participate in the crosslinking of the AESO monomer, drawing for the carbon black particles a tridimensional conductive network in which they are well distributed and dispersed. To overcome the inconvenient of processing the polyAESO composites one option was to copolymerize the AESO with other acrylic monomer as butylmethacrylate (BMA). Polymer from BMA is not a rigid polymer as polystyrene or poly(metylmethacrylate) but it contains a carbonyl group as ASEA and a short alkyl chain enough to be miscible with ASEA. After studying the electrical behavior and evaluating the critical fraction of the polyAESO and polyBMA both with CB particles, rendered values of 4 and 14%CB respectively. It was established to copolymerize both monomers, ASEA and BMA, in order to improve the processing properties and to evaluate the changes in the electrical properties respect the composites based on the respective homopolymers. Considering the great difference in the critical fraction values of polyASEA and polyBMA composites it was expected that this value was dependent on the comonomers proportion. In order to establish one only proportion it was necessary to do a scanning on the composition vs resistivity property maintaining constant the CB load which was chosen as 10 wt% CB. Once the percolation curve (Figure 3 in reference 17) was built it could be appreciate that as increased the ASEA load in the range of 0 to 10%, the resistivity decreased sharply (seven orders of magnitude) until it reached a minimum and constant value. From these results it was chosen a copolymer composition of 30:70 wt% of ASEA/MAB, taking in account that a higher quantity of ASEA produces processing problems. The results will be discussed later in section 2.1.2.

Another interesting option was to copolymerize the ASEA with another commercial modified natural-derivate comonomer named (Acrylamidomethyl) cellulose acetate butyrate (ACAB). This semicrystalline polymer is a cellulosic product soluble in organic solvents and also it is crosslinkable by free radical reaction. It is well know that cellulose is the most abundant naturally occurring organic substance which is very insoluble and its products are extensively used in non-food and industrial applications mainly as textile, paper, thickeners, flocculants, etc. Many derivates have been synthesized in order to synthetic polymer replacements, being

hydroxyl groups in cellulose the most available source of chemical modification that has been exploited. For example, cellulose esters and ethers, which usually are water-insoluble, have been used as plastics for molding, in modern coatings, extrusion, laminates, controlled release of actives, biodegradable plastics, composites, optical films, and membranes and related separation media [82, 83]. ACAB was synthesized in order to have not only esters and ether functionalities, but also polymerizable vinyl functionalities by react the hydroxyl cellulosic groups with N-metilolacrilamide [84].

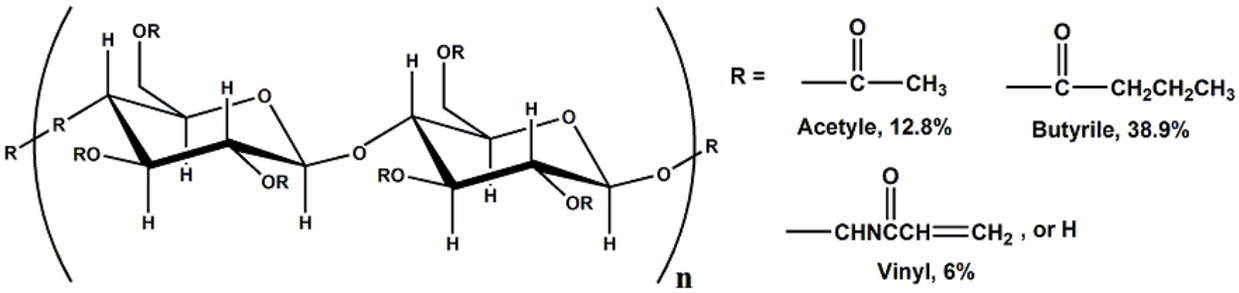

Figure 3. Structural representation and composition of commercial ACAB.

Polymerization and copolymerization could carry out by thermal, ultraviolet, gamma or electron beam radiation. It contains in average the next composition (Figure 3): 38.9% of butyril groups (~1.8 mol butyrate per mol cellulose), 12.8% of acetyl groups (~1.0 mol acetate per mol cellulose), and 0.6% of vinyl ones (~0.1 mol vinyl per mol cellulose). It is a white powder useful for produce crosslinked and insoluble resistant copolymers, hard, durables as adhesives and composites in the textile industry, to provide articles which should retain a permanent shape. Coatings are effective on wood, paper, metal, plastics and they are useful to produce containers, furniture, floors, appliances, trucks, pipe, boats, paper products, among others. Recently ACAB was used to produce columns with higher separation efficiencies of aminoacids and peptides by capillary electrochromatography [85].

Considering the good processing properties of ACAB, the miscibility with AESO, the great number of polar groups and the presence of a vinyl crosslinkable functional group, were the reasons to establish this study in which the main goal is to obtain processable conductive composites and with low critical fraction. In this study three types of CB particles were used. The properties and methodology are described in section 2.2.

The possibility to generate polymer composites from natural sources monomers with modified electrical properties is of high interest due the mentioned reasons and for the possibility of reduce the critical fraction. As mentioned before the preparation methodology is very important in order to obtain a very good CB dispersion and reproducibility of the electrical properties. The next section will be devoted to describe the preparation of the AESO-co-BMA and AESO-co-ACAB copolymers and the respective composites with CB´s as well as the characterization of products by FT-IR spectroscopy, Differential Scanning Calorimetry (DSC) and Thermogravimetric Analysis (TGA).

http://dx.doi.org/10.5772/52992

2. Detailed description for obtained copolymers and their structural and thermal characterization

2.1. System AESO-co-BMA

2.1.1. Reactants and equipment

The used reactants in this section are described: AESO containing in average 3.4 acrylates per molecule, and contains 4,000 ppm of monomethyl ether hydroquinone (MEHQ) as inhibitor; density 1.04 g/mL at 25°C. BMA (99%) comonomer contains 10 ppm of MEHQ; bp. 162-165°C, density 0.894 g/mL at 25°C. Potassium Bromide, KBr was spectroscopic degree; Tetrahydrofurane (THF) (99.7%), bp. 70°C; and Acetone (99%) both as solvents. All of them were purchased from Sigma-Aldrich, Co. Dibenzoyl peroxide (BPO) (> 97%), mp 102-105°C, was purchased from Merck Co; and Carbon black Vulcan X-C72 was kindly donated by Cabot Co. Before use, ASEA and BMA were surpassed by an inhibitor-remover packing (from Sigma-Aldrich, Co) in order to remove the MEHQ. Other reactants were used as received.

For Infrared characterization a FT-IR Nicolet Avatar 360 was used. All samples were mixed with previously dried KBr and pressured at 8 Tons in order to obtain transparent plates. 32 scans were recorder from 4500 to 400 cm^{-1} at a resolution of 8 cm^{-1}.

For calorimetric characterization, a SDT Q600 modulus (TGA coupled to a DSC) from TA Instruments was used. Experiments were recorder at a heating rate of 10°C/min, under nitrogen atmosphere (100 mL/min), from 23 to 500°C.

2.1.2. Synthesis and characterization of pure AESO-co-BMA copolymer, 30/70 wt%.

The pure copolymer is obtained following the next methodology, using as example 1g of total prepared compound: 0.3 g of ASEA is weighed into a 150 mL round bottom flask and 10 mL of THF are added. The mix is sonicated in an ultrasonic processor (Ultrasonik™ 28X 50/60Hz) at 5-8°C for 10 min until ASEA is completely solved. Then 0.7g (0.78mL) of BMA is added in junction with 0.05 mL of 0.5M PBO in THF and again the mix is sonicated for 2 min only, at same temperature. After, a condenser with inlet and outlet nitrogen ultrapure gas (from Infra, Co) is adapted to the flask. It was left the low nitrogen flux for 5 min and finally the temperature is increased from room temperature (RT) to 70°C in order to copolymerize. Copolymerization takes around 6 hr and it can be detected because the copolymer starts to precipitate due to the crosslinking reaction. Once the product is precipitated as several pieces, the temperature is lowered to RT, the nitrogen is turn off and the transparent lightly yellow product is filtered and washed twice with acetone to remove the possible residual monomers and initiator. The copolymer is well dried under vacuum for 24 hr. This copolymer is characterized by FTIR spectroscopy, detecting specific signals for both comonomers. Finally, the greatest piece was cut into a cylinder shapes (1.0 cm diameter x 0.2 cm thickness) and the faces were covered with silver paint in order to measure the resistivity.

For a structural characterization of the copolymer by FT-IR spectroscopy, it is necessary to know the main absorption bands of the monomers and homopolymers, in this case for MAB,

polyMAB, AESO and polyAESO. For BMA, the next bands are identified: vinyl bond (=C-H) from acrylic group is found at 3100 cm^{-1}, methyl and methylene groups (-CH3-, -CH2-) between 2900 cm^{-1} and 2800 cm^{-1}, carbonyl (C=O) from ester group at 1743 cm^{-1}, polymerizable double bond (-C=C-) from acrylic group is sited at 1640 cm^{-1} and another vibration related with end double bonds (H2C=) also from acrylic group is sited at 950 cm^{-1}. When BMA is polymerized (Figure 3), the main changes on the respective spectrum are: the diminishing of the bands corresponding to the double bonds at 3100 cm^{-1}, 1650 cm^{-1}, and 950 cm^{-1}. These absorption bands diminish in intensity as the polymerization take place and finally they disappear when polymerization has been completed.

For AESO monomer (Figure 4) the most important identified bands are: Hydroxyl (-OH) groups at 3500 cm^{-1}, vinyl group (=C-H) from acrylic one at 3100 cm^{-1}, methyl and methylene groups (-CH3-, -CH2-) between 2900 cm^{-1}, 2800 cm^{-1}, carbonyl vibration (C=O) from esters groups is sited at 1730 cm^{-1}, double bonds (C=C) from the acrylic pendant groups are found at 1650 cm^{-1}. Finally, at 750 cm-1 is sited the typical band due to four or more continuous methylenes (-CH2CH2CH2CH2-…) from the fat acids chains. The main changes observed when ASEA is polymerized to polyASEA (Figure 4) are those related with the acrylic double bonds at 3100 cm^{-1} and 1650 cm^{-1}. As the same as BMA polymerization, those bands decrease in intensity as polymerization takes place; at the end of polymerization they are no detected. All the other signals practically do not change.

For copolymer ASEA-co-MAB (Figure 4) the main information obtained from the FT-IR spectra are that signals of both monomers are seen overlaid and the main ones are those corresponding to the acrylic double bonds. It is logic that they are not detected by copolymerization; however there are still small signals corresponding to acrylic double bonds of the BMA at 1632 cm^{-1}, even after washing the product with THF. BMA monomer was not detected in the filtered THF after remove the solvent. That indicates that it does not correspond to an incomplete reaction of BMA (residual monomer). The small double bonds signals seen on the spectrum are attributed to a higher load than ASEA, generating segments of BMA units with disproportion ends chains.

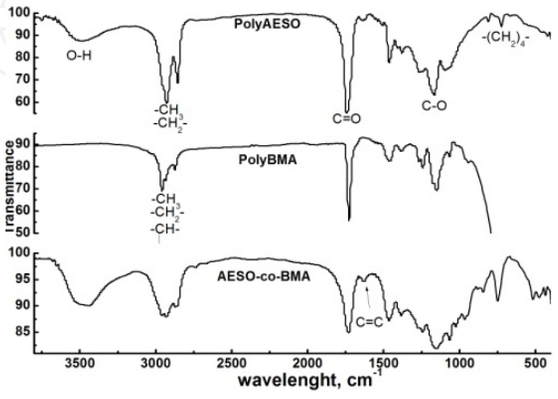

Figure 4. Comparison of the IR absorption bands for polyAESO, polyBMA and AESO-co-BMA

http://dx.doi.org/10.5772/52992

The FT-IR study is not determinant to corroborate if there was a copolymerization, however the thermal properties indicates that there is. DCS/TGA analysis also were made in order to found a possible transition and to determine the decomposition temperature considered it at which de polymer lost the 10 wt% (T_{10}) of its original weight percent. By DSC, ASEA monomer shows an exothermal crosslink curve with a maximal temperature at 349°C and immediately the decomposition is observed. TGA shows that ASEA´s T_{10} is detected at 360°C in one step. Once the ASEA is polymerized, the DSC curve does not show any transition: no residual exothermal curve due to crosslinking, neither T_g indicating a complete polymerization under the described conditions. There is difference in the T_{10} in 7°C lower for polyASEA in comparison with ASEA monomer. This decreasing is explained in terms on that crosslink decreases the free movement of the fat acids arms on the polyASEA in such a way that heating tends to break that inter-chain tension at lower temperatures. The T_{10} of polyBMA was detected at 230°C. The T_{10} of the copolymer is 302°C which is lightly next to the polyASEA value (Figure 5) due to the crosslinking reaction between both monomers, even BMA is in major proportion. Decomposition of the copolymer occurs in only one step, indicating the product is only one compound (copolymer) without byproducts such as homopolymers or oligomers.

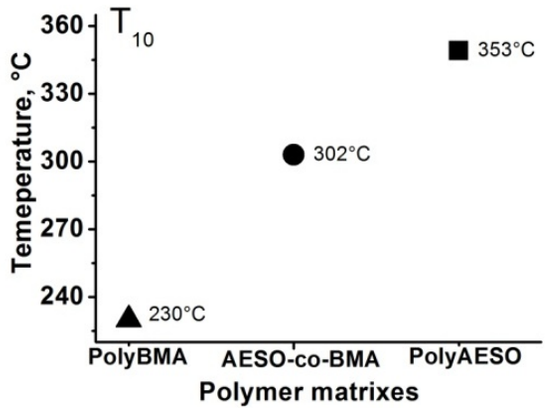

Figure 5. Decomposition temperature (T_{10}) for AESO-co-BMA copolymer and its respective homopolymers: polyAESO and polyBMA

2.1.3. Preparation and characterization of AESO-co-BMA copolymer composites with carbon black

For preparing composites based on ASEA-co-BMA and CB particles, it is followed the next methodology which is similar as the described for pure copolymer synthesis. Composites preparation starts with the dissolution of 0.3 g of ASEA monomer in 20 mL of THF and then the addition of 0.78 mL of MAB monomer. At this homogeneous mix is added the corresponding amount of CB depending on the composition to prepare. In this case were prepared the next CB loads: 0.5, 1.0, 1.2, 1.3, 1.4, 1.5, 2.0, 2.5, 3.0, 3.5, 4.0, 6.0, 8.0, 9.0, 10.0, 15.0 and 20.0 wt% CB. The mix lefts to disperse by sonication for 2 hr at 8°C. Finally the same milliliters of initiator solution is added, nitrogen flux is adapted and the composite is left to polymerize at 70°C for 4 hr and then at 95°C for 2 hr. The composites precipitate as a black unshaped mass; they

are washed three times with acetone and filtered in order to remove the probable residual monomers and/or initiator. Finally they are dried under vacuum for 48 hr.

Respect to the composite characterization by FT-IF spectroscopy, the spectra are very similar to the pure copolymer with only one difference, the signals corresponding to the graphitic structure of CB, composed by double bonds C=C sited at 1633 cm^{-1} increases subtle as the CB load do. Referent to the thermal properties, T_{10} of the composites based on ASEA-co-BMA depends on the CB load. For example, for 0.5 wt% CB a T_{10} of 342°C is detected, whereas for 6 wt% CB the T_{10} is 335°C. Is a fact that CB acts as thermal reinforcing filler in this matrix however, that reinforcement decreases as the CB load increases. This is one reason for the interest in produce composites with low critical fraction, usually as the CB load increases some other properties as mechanical or processing ability tend to decrease as well the potential applications as sensing.

It was not a successfully improvement of the processability by copolymerize AESO with BMA, copolymer and the respective composites were insoluble, unmelted, and the thermomolding process was not possible, nevertheless it was obtained a very low critical fraction (1.2 wt% CB) [17].

2.2. System AESO-co-ACAB

In this section the electrical properties of polymer composites based on (Acrylamidomethyl) cellulose acetate butyrate, ACAB, and its copolymer with acrylate-epoxidized soybean oil (AESO) (50:50 wt%) are discussed. Three different commercial carbon black (CB) particles were used in this study: Raven 5000, Vulcan XC-72 and N660 which have different properties as size, structure (ramification percent), oxidize surface and conductivity (see Table 1).

2.2.1. Reactants and equipment

Commercial (Acrylamidomethyl) cellulose acetate butyrate, ACAB has a Mn of 10,000, mp 155-165 °, Tg 118°C, density 1.31 g/mL a 25°C, it is soluble on a variety of acrylic monomers. Benzophenone photoinitiador, BPN (> 99%), mp 47-51°C, both were purchased from Sigma-Aldrich, Co. Reaven 5000 and N660 CB´s particles were kindly donated by Professor Wiltold Brostow from UNT, USA. All of them were used as received. For electric contacts silver paint SPI 18DB70X was purchased from Electron Microscopy Sciences. Some properties of the carbon blacks particles are shown in Table 1.

Carbon particles have many different properties according to the raw reactants and on the synthesis method. They are into the 50 chemical products more produced in all around the world and actually, CB particles are the result of an incomplete combustion from hydrocarbons. 90% of CB is useful as reinforcement particles in elastomers for fabrication of wells, 9% as pigment and the rest 1% in other specific applications as paints and electric devices [86]. Additional to their stain power, their electric or charge action provide UV radiation protection to the polymers at low cost. The CB particles are constituted from almost spherical particles with a graphitic structure (electrically conductive) and colloidal dimensions. Their structure consists in many primary nanoparticles (from 10 to 100 nm) bonded into a bunch named "aggregate" with dimensions from 50 to 500 nm. Those aggregates use to form macro-

agglomerates with more than 1μm of size [1]. CB aggregates have different shapes, they could be 1) spherical, 2) elispsoids, 3) lineal or 4) branched. Chemically are constituted from 83% to 99% of elemental carbon and according to the fabrication method it could be founded many oxygenated functional groups as phenols, quinolics, carboxylics, etc. on the surface. This is related to the ash content which is usually less than 5%. For electrical properties, are required that CB particles have branched structures (high structure), an oxidized surface which allows to disperse them into several polymer matrix, a high diameter and good intrinsic electrical conductivity. Branched structures as in CB Vulcan X-C72 allow a large contact number or electronic sits for build the conductive paths with a lower load of conductive particles. Opposite to this, CB N660 has the lowest structure and superficial area but a particle diameter of 50 nm and a structure manly lineal. CB Raven 5000 particles show a low structure and superficial area but have a highly oxidized surface in comparison with the others. Their resistivities [see section 3.1] are not so different making interesting to study how the other mentioned properties have influence in reaching the percolation threshold at low critical fractions.

CB Particles	Average diameter size, nm	Volatile % (oxidized surface)	Branched structure, %	Resistivity (cm)
Raven 5000 Ultra II [87]	8	10.5	45.5	1.1
Vulcan XC 72 [86, 88]	32	< 2	77.3	0.08
N660 [89]	50	2.5	31.7	0.19

Table 1. Characteristics of the three used carbon black particles

The FTIR spectra for the three different types of CB, shows the same superficial functional groups, being the only difference the intensity of the signals (Figure 6). Those characteristic absorption bands are: hydroxyls groups (O-H) from 3416 cm^{-1} a 3440 cm^{-1}, methylene (C-H) from the amorphous CB composition at 2923 cm^{-1} y 2850 cm^{-1}; carbonyl bond (C=O) due to different groups as esters, carboxylic acids and quinones are seen from 1709 cm^{-1} to 1740 cm^{-1}; typical vibrations of the double bonds (C=C) that constitute the graphitic composition of the different CB´s are sited from 1578 cm^{-1} to 1632 cm^{-1}; this due there are some double conjugated bonds with carbonyl group from quinones. A combination of vibrations due to the C-O and O-H from esters and phenols, respectively are founded at 1380 cm^{-1} and 1216 cm^{-1}; finally are seen a combination of vibrations for C-O bond from hydroxyl groups in phenols at 1064 cm^{-1} y 1066 cm^{-1}. At 680 cm^{-1} is sited an out of the plane deformation vibration for O-H bond which is only seen in CB N660.

2.2.2. Synthesis and characterization of crosslinked ACAB ($_{cross}$ACAB)

This reaction was neccesary to know and stablish the copolymerization reaction conditions and the processing properties. For pure crosslinked ACAB, 1 g of ACAB is weighed into a 150 mL round bottom flask, 10 mL of THF are added and the mix is sonicated for 15 min until the

complete dissolution of ACAB. At this point 0.05 mL of a 2.0M THF solution of PBO is added and shaking another 2 min. The condenser and the nitrogen atmosphere are adapted to the flask and the temperature starts to increase from RT to 70°C as a first step. The crosslinked ACAB ($_{cross}$ACAB) starts to precipitate. After 5 hr of reaction, the temperature increases from 70 to 88-90°C for 4hr in order to finish the crosslinking reaction. Heating and nitrogen gas are turn off and at RT and the transparent one piece polymer is washed twice with acetone en order to remove residual ACAB and/or initiator. Finally it was well dried under vacuum for 24 hr. The polymer was cut in small pieces and they were processed by thermo mechanic technique. This allowed preparing cylinders of 1.0 cm diameter x 0.2-0.3 mm thickness in order to measure the resistance.

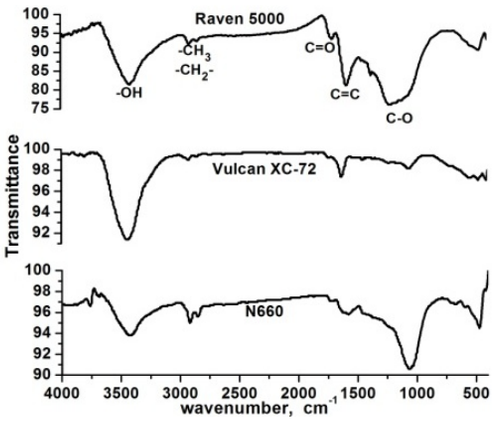

Figure 6. FI-IR spectra if the three types of used CB particles: Raven 5000, Vulcan XC-72, N660

The characterization of ACAB by FTIR spectroscopy allows distinguishing the next important signals: Hydroxyls and amide (–O-H, –N-H) vibrations appear at 3700-3250 cm^{-1}; methyl and methylene vibrations (C-H) from of the polysaccharide ring are sited at 2970 and 2879 cm^{-1}; carbonyl vibration (C=O) from ester groups (acetate and butyril) are found at 1750 cm^{-1} and at 1679 cm^{-1} it is possible to distinguish the carbonyl vibration from amidomethyl group. Double bond band (C=C) is sited at 1630 cm^{-1}, and the corresponding terminal double bond ($C=CH_2$) is at 919 cm^{-1}. Signals monitored in order to found the time in which ACAB completely crosslinks are those corresponding to the vinyl group, 1630 and 919 cm^{-1}. The $_{cross}$ACAB is characterized by FTIR spectroscopy detecting the disappearance of those mentioned signals (Figure 7).

Concerning with the thermal properties, it was interesting to note that the decomposition temperature, in this case taken as the onset temperature (T_{ons}) due some little lost before decomposition temperature due to humidity or some remnant solvents in case of $_{cross}$ACAB. Those temperatures were very similar with a difference of 2°C higher for $_{cross}$ACAB respect to the ACAB. This slightly difference could be due to the small amount of crosslink vinyl groups (only 0.6%) which not do much difference in that property. The DSC thermogram for both compounds does not show differences, it is possible to distinguish an exothermal curve with a maximal temperature at 145°C that encloses both the T_g and the T_m reported transitions. This

http://dx.doi.org/10.5772/52992

is one reason for which polyACAB shows processability under temperature and pressure and is possible to soften or melt in order to mold it to any required shape, which was something expected.

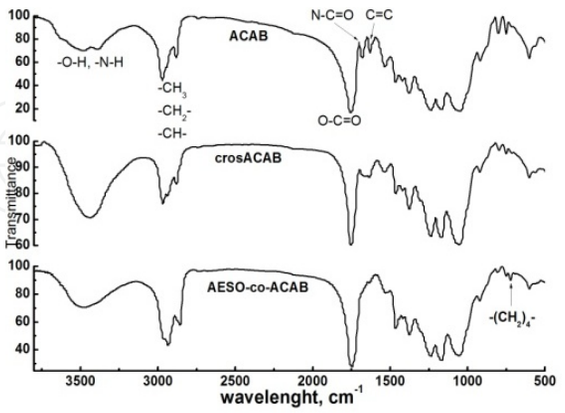

Figure 7. FT-IR spectra for ACAB, $_{cross}$ACAB and AESO-co-ACAB polymer matrixes

2.2.3. Synthesis and characterization of the pure copolymer, AESO-co-ACAB (50/50 wt%)

For preparing 1g of AESO-co-ACAB (50:50 wt%), 0.5g of ACAB are weighed into a round bottom flask, 5 mL of THF are added and it was solved into an ultrasonic processor for 15 min. Then 0.5 g of ASEA and 5mL more of THF are added to the last mix and again homogenized into the ultrasonic processor for 10 min. The same quantity of PBO initiator as the described polymerizations is added and all mix is copolymerized following the same procedure described for $_{cross}$ACAB. The reaction for this system needs 7 hr for polymerizes at 70°C, and then the temperature is increased to 88-90°C for 4 hr. The product as a one translucent and lightly yellow homogeneous piece which is filtered and washed three times with acetone and finally dried under vacuum for 24 hr. This product, softer than $_{cross}$ACAB also shows processability by thermo molding being one of the main goal of this proposed system.

The FT-IR spectrum shows absorption bands of the two comonomers and the most characteristics are: 1535 cm^{-1} (C-H and N-H), 755 cm^{-1} (N-H) from the amide group. 1601 cm^{-1} (C=O) it is a vibration from all esters in both monomers. The most representative band for ASEA is at 723 cm^{-1} which is typical for more than four continuous methylene groups. There is not band sited at 1634 cm^{-1} corresponding to double bonds indicating a complete copolymerization between both monomers.

The TGA analysis of the copolymer indicates two lost, one of 2% before the 150°C due to remnant solvent and humidity and a second at 351°C which corresponds to its decomposition. Figure 8 shows the decomposition temperature of the three pure polymer matrix. As we can see, the decomposition temperature for the copolymer is in the middle of the homopolymers. Taking in account that the decomposition occurs in only one step, it becomes and evidence that copolymerization between ACAB and ASEA took place.

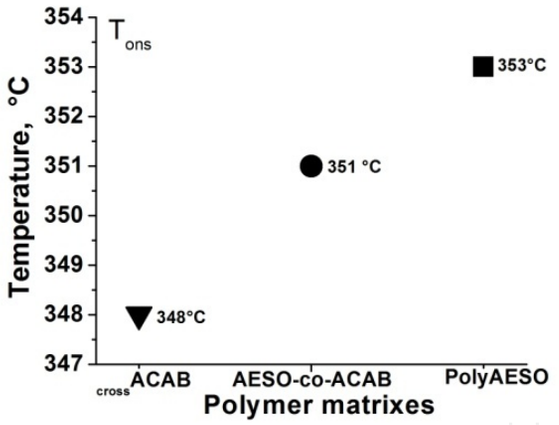

Figure 8. Decomposition temperature of the three polymer matrix: $_{cross}$ACAB, AESO and AESO-co-ACAB (50:50 wt%) copolymer

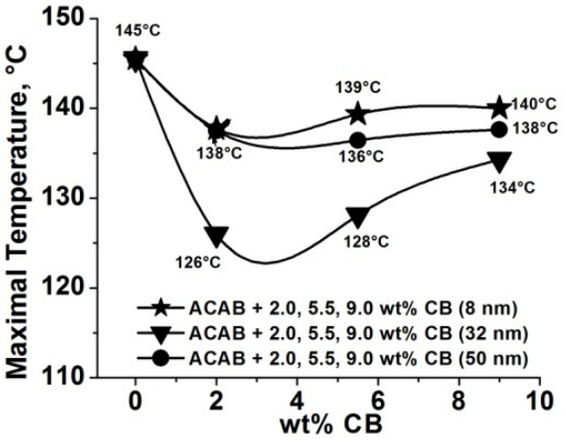

Figure 9. Changes on maximal T_{gm} according to the type and amount of CB particles

The DSC curve showed a diminishing curve due to the melting point of ACAB matrix (145°C), but it does not show any residual exothermal curve due to the ASEA cure. These events suggest that the copolymer could be processable by thermomolding thanks to the thermoplastics properties imparted by the ACAB polymer.

2.2.4. Preparation and characterization of AESO + CB particles

The CB compositions for composites based on ACAB with CB, independently of the type of CB, are: 1.0, 2.0, 2.5, 3.0, 4.0, 4.5, 5.5, 7.5 and 9.0 wt% CB. An example is described for preparing 1g of composite with 1 wt% CB. 0.99 g (90 wt%) of ACAB is solved in 30 mL of THF by sonication for 10 min into a 150 mL round bottom flask and 0.01g (1.0 wt%) of CB is added. The mix is sonicated for 2 hr until a homogeneous solution is observed. At this moment the solvent is distilled with a rotovapor and finally the solid mix is well dried under vacuum for 24 hr until a black powder is obtained. For the other compositions the methodology was the

http://dx.doi.org/10.5772/52992

same, the only difference is the dispersion time: 2 hr for 1.0 to 4.0 wt% CB and 4hr to 4.5 to 9.0 wt% CB.

When CB is dispersed in ACAB or into de copolymer, the detection of CB particles by FTIR is the same in any case. Here is exhibited the analysis only with the copolymer and CB Vulcan XC72: the absorption band a 1632 cm^{-1} which correspond to graphitic CB zone (C=C) or 1582 cm^{-1} for 8nm-CB, is subtle increased as the CB load increases. There are other bands which overlayer the composite spectra. At 3416 cm^{-1} - 3440 cm^{-1} we have a vibration for (O-H) hydroxyl functional group, at 2923 cm^{-1} and 2850 cm^{-1} are the vibrations corresponding to the amorphous zone of the CB's (C-H). From 1709 cm^{-1} to 1740 cm^{-1} appear the vibrations of C=O bond corresponding to esters groups; at 1578 cm^{-1} a 1632 cm^{-1} are the vibrations of the graphitic composition of the CB's particles which correspond to C=C conjugated with carbonyl group from quinones. At 680 cm^{-1} we have a bending vibration of the O-H bond out of plane which is only observed in CB N660.

In Figure 9 was plotted a temperature (T_{gm}) which encloses the Tg and maximal T_m for ACAB matrix in composites with 2, 5.5, 9 wt% CB, identifying the next information: All ACAB-based composites show a diminishing on the T_{gm} respect to pure ACAB. An explanation is that CB particles act as impure or lubricant, abating both temperatures, mainly the T_m as observed for other authors [90]. The higher effect is shown when CB N660 is used.

On the other hand, respect to the decomposition temperatures, shown in Figure 10, it can be seen that the addition of any CB used particles tends to increases the decomposition temperature respect to the ACAB matrix (346°C). In Figure 10 only T_{ons} for three compositions are plotted: 2, 5.5 and 9 wt% CB. The smallest CB particles (8nm) give the composites with the higher decomposition temperatures around 351°C, followed by those based on 50nm-CB (N660) which have T_{ons} around 348°C and finally those particles that almost do not have a great effect on the decomposition temperature were the 32nm-CB particles, maintaining it around 346.5°C.

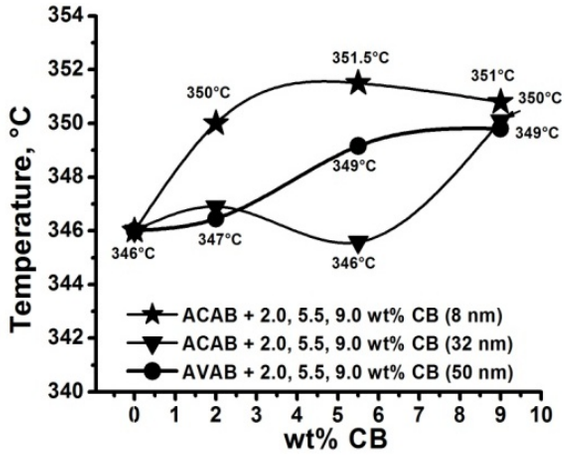

Figure 10. Decomposition temperatures for ASEA+CB composites as a function of the type and amount of the CB particles

The incorporation of the CB particles increases the decomposition temperature of the composite, it could be due to that intermolecular interaction seems to be favourable between the functional groups of the polymer matrix and those of the CB particles [1]. It is important to take in account that 8nm-CB particles have a higher oxidized superficial area implying a great number of hydroxyl and carboxyl groups that could render hydrogen bridges with those on the ACAB polymer. It is because composites prepared with 8nm-CB have a higher resistance to decompound thermally. However 50nm-CB particles have scarce superficial functional groups and less superficial area and in turn negligible interaction with the polymer matrix and a less decomposition temperatura for the respective composites. An intermediate case is for ASEA+ 32nmCB composites.

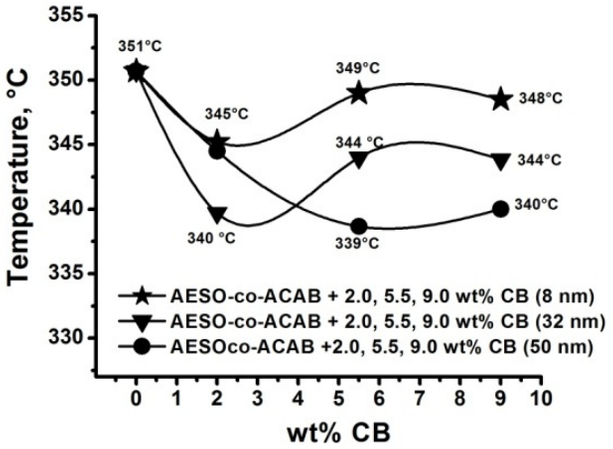

Figure 11. Decomposition temperature for the copolymer composites base don AESO-co-ACAB as a function on the type and amount of CB particles

2.2.5. Preparation and characterization of AESO-co-ACAB + CB´s composites

The preparation of these composites also is also via free radicals. For 32 and 50 nm CB´s, thermal initiator decomposition was used, but for CB Raven 5000 (8nm) was necessary to use the photochemical method via benzophenone/UV radiation as initiator system. The reason is that was not possible to obtain composites via thermal decomposition. A possibility is that some superficial groups on CB Raven 5000 act as inhibitors or quenching free radicals consuming them. In case of UV radiation, it is possible to reactivate the apparently inhibited free radicals. This could be supported by the fact that those copolymer composites were cured under air atmosphere, not under nitrogen flux as in thermal copolymerization.

The CB compositions prepared for these systems were the same as those described for ACAB: 1.0, 2.0, 2.5, 3.0, 4.0, 4.5, 5.5, 7.5 and 9.0 wt% CB. In the copolymer composites,the CB load was calculated considering 1 g of comonomers in which 0.5 g of ASEA and 0.5 g of ACAB are used for synthesize the copolymer matrix. The first stage of the preparation is the same independently of the type of CB used: First 0.5 g of ACAB are weighted and solved in 30 mL of THF by

http://dx.doi.org/10.5772/52992

ultrasonic shake for 10 min. 0.5g of ASEA are added and sonicated again for 10 min in order to get a homogeneous clear solution. Then the respective amount of CB is added (depending on the composition) and the mix is sonicated for 2 or 4 hr (as same as ACAB composites). Finally, depending on the initiator system, when 8nm-CB is added, 0.01 mL of 0.2M BPN in acetone is dropped and sonicated 2 min more. The mix is poured into a glass mold covering the bottom. The solvent is slowly evaporated inside an extraction bell in such a way that composite mix forms a homogeneous layer. The glass mold is put into a CL-1000 ultraviolet-crosslinker UVP (with a maxima wavelength of 254 nm) and copolymerized at 720 J/cm^2 for 4 hr. The composites are obtained as a solid layer with a shining black aspect, which is insoluble in water and organic solvents. The composite layer is collected and reserved.

When CB of 32 and 50nm are used, 0.05 mL of 2.0M PBO in THF is added, and following the same methodology as in pure copolymer, the mix is cured at 70°C for 5h and then a 90°C for 2 hr under nitrogen flux. The cured composite precipitate as black solid pieces which are filtered and washed twice with acetone and dried under vacuum for 24 hr.

By FT-IR spectroscopy, as the same to the aforementioned for the ACAB composites, the only effect is the increasing of the band at 1632 nm which corresponds to the double bonds of the graphitic composition in CB particles. The same effect is observed in all copolymers and that signal seems to increase as the wt% CB does.

Concerning with the thermal properties of copolymer composites only was detectable the decomposition temperature, it was very difficult to detect some T_m surely due to the addition of CB particles which influence the possibility to crystallize and T_g was not evident. But TGA analysis shows interesting results, in the case of the copolymer matrix the effect on the T_{ons} is opposite to that analyzed for the ASEA polymer (Figure 10). In copolymer composites at 2, 5.5 and 9wt% CB's, the T_{ons} is diminished with the CB particles addition respect to the copolymer matrix. 8nm-CB particles seem not to have an important effect on the decomposition temperature, except for 2 wt% CB in which the temperature is reduced from 351°C (copolymer) to 345°C. At this same CB composition, 32 nm particles show the stronger effect on T_{ons} diminishing it at 340°C, but with the increasing of the CB load, the reached value for T_{ons} was in average 344°C. The 50nm-CB particles had its more critical effect at 5.5 wt% CB decreasing the T_{ons} from 351 to 338°C.

3. Electrical properties evaluation

3.1. Electrical properties of carbon black particles

In order to compare the electrical properties of the different prepared and characterized polymer composites, the electrical properties of the three types of carbon black were determined under the same conditions [91, 92]. Each type of CB was hydrostatically compressed into a system which consists of a cylinder-piston couple, as shown in Figure 12 and the electrical resistivity was calculated using the relationship 2.

$$\rho = R\frac{A}{l} \tag{2}$$

Where the electrical resistance R was measured with a LRC720 Stanford Research System. The length of the compacted particles l, and the transversal section area A were measured with a micrometer and a Vernier respectively. The same amount (100 mg) and pressure (20 Kg/cm^2) were applied to the three CB particles. Cupper electrodes of 6 mm diameter, 1cm length for the inferior and 2.5 cm length for the superior one were used. The electrical resistivities are shown on Table 1. As it can be see, the Vulcan XC-72 have the lowest resistivity and Raven 5000 the highest indicating that the most conductive CB is the Vulcan XC-72.

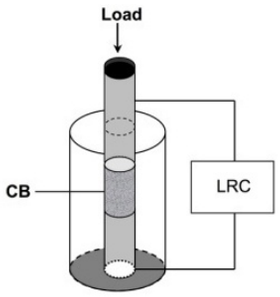

Figure 12. Design for measure the resistance of the CB particles

3.2. Percolation curves and percolation threshold calculus for composites

For composites based on AESO-co-BMA, the methodology for electrical measurements is well detailed in reference [17] and the most interesting results were the low critical fraction of both composites based on polyAESO and on the AESO-co-BMA matrixes, 4.0 and 1.2 wt% CB, respectively. These results will be discussed on section 3.3.

For the other systems (ACAB, AESO-co-ACAB) the electrical treatment is described: Polymers composites were processed by thermo-molding technique at 1.5 MPa in order to get samples of 1.2 cm diameter and 2 mm thickness [81, 93]. The processing conditions of temperature and time are summarized in Table 2 and those conditions depend on the polymer matrix. The bulk resistivity was determined using the two-points technique and silver paint (SPI de Electron Microscopy) as electric contacts were put on the parallel faces of the composite samples.

The voltage-current relationship is measured with a Keithley 6517A electrometer [17, 81, 93]. For each composition the resistivity was calculated via the relation 2 building the respective percolation curves in a width range of compositions. As an example, the percolation curves for AESO-co-ACAB are exhibited in Figure 13. From these curves and using Origin 6.0 software the percolation threshold and the critical fraction are numerically calculated fixing the experimental data to the equation 1. As we can see, the critical fraction for polymer composites based on ACAB and AESO-co-ACAB is modified due to the CB particles as well as the polymer matrix.

Polymer composite	Temperature/ °C	Compression time /min
ACAB	122	30
ASEA/ACAB	118	40

Table 2. Processing conditions of ACAB and ACAB-co-AESO composites

For the ACAB composites the critical fraction varies from 2.8 to 7.5 wt% CB whereas the AESO-co-ACAB copolymer composites the respective values are from 2.4 to 3.2 wt% CB (Figure 14). This demonstrates that polymer matrix influences the electrical properties of the final composite. However in terms of CB properties, the decreasing of the critical fraction with a increasing of the CB structure converges very well with the percolation theory. As we discussed before, when are used aggregates with small particles and low structure it tend to need more particles in order to interconnect them and to build the electrically conductive paths, in comparison with high structure and bigger particles (as Vulcan XC-72 respect to Raven 5000). Also, other CB properties as intrinsic resistivity are evident. For both systems the CB particles with the highest resistivity (Raven 5000, 8 nm) are those with a higher critical fraction.

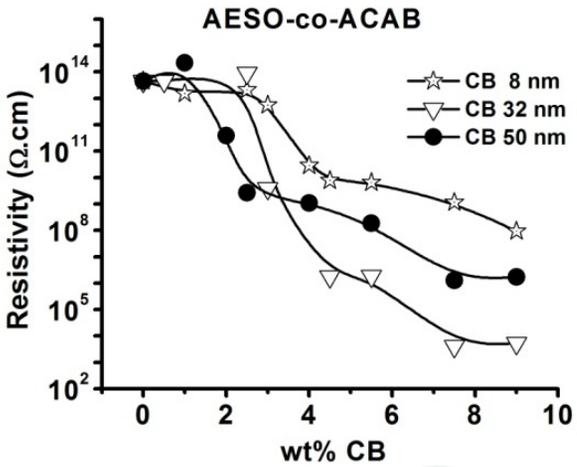

Figure 13. Percolation threshold of the AESO-co-ACAB composites for different carbon black particles

3.3. Analysis of electrical properties as a function of carbon black particles and polymer matrix nature

From the results we could discuss that the chemical nature of the polymer matrix as well the CB properties contribute to the disaggregation, dispersion and preferential distribution of the conductive particles into the polymer matrix. However it is possible to control the preferential build of conductive paths and diminishes as a consequence the critical fraction? As was mentioned before, there are some successfully attempts for controlling it but only oleo-polymer has been used for that and critical fraction lower that 3% are not obtained yet. However, AESO has become a question in to decrease the critical fraction under copolymerization. For the system AESO-co-BMA, a very low critical fraction of 1.2 wt% CB was calculated. Something

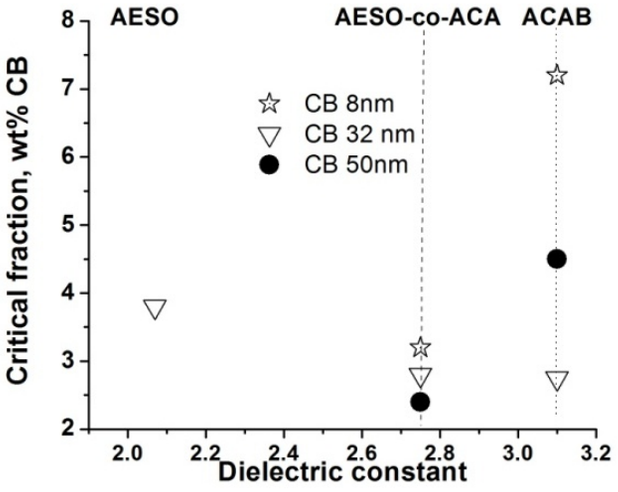

Figure 14. Critical fractions respect to the type of CB and to the polymer matrix

similar is observed for the AESO-co-ACAB composites. If we analyze the critical fractions on Figure 15, we could appreciate that copolymers composites have the lowest critical fraction independently on the type of CB particle. For oleo polymers, in a systematic work [16] was demonstrate that the dielectric constant of the polymer matrix is directly associated with the critical fraction. Due to the unprocessability of the AESO-co-BMA copolymer it was not possible to measure the dielectric constant but it was made for ACAB, AESO and the AESO-co-ACAB matrixes (Figure 15). For dielectric constant polymers were processed into disks of 2cm diameter x 0.9-1.1 mm thickness by compression molding. An Agilent 4991 A RF impedance/Material Analyzer at 450 MHz and room temperature [16].

We can realize that AESO has the lowest dielectric constant (2.1) whereas ACAB has the highest one (3.1). Even both molecules have polar groups; the AESO has large alkyl chains also, whereas ACAB has oxygen as constituent of different functional groups being carbonyl and hydroxyl the main. Unsurprising constant dielectric value for the copolymer was obtained in 2.7. The tendency with CB Vulcan XC-72 is the same as the reported results on [16]: at a highest dielectric constant, a diminishing in the critical fraction is observed. The amazing results are in the low critical fractions for the copolymer composites (from 2.4 to 3.2) with the three types of CB particles in comparison with the ACAB composite which possess the highest dielectric constant. These results claim that the dielectric constant is important to take in account however the role of the AESO is completely understood but definitively it tends to low the critical percolation. From the structural point of view, polyAESO is an amorphous and 3-D crosslinked polymer while AESO is a semicrystalline and lineal one. However when AESO crosslinks builds a bonds network with polar groups thanks to the reaction of the acrylic groups. This network draw preferential paths (in blue, Figure 16) for a good dispersion and distribution of the CB particles without have to fill the entire matrix. In conjunction with the polar functional groups of the other comonomer, very low critical fractions are reached under copolymerization with BMA and ACAB. The differences on the critical fraction will surely dependent on the CB properties as the size, structure, surface and the intrinsic conductivity.

http://dx.doi.org/10.5772/52992

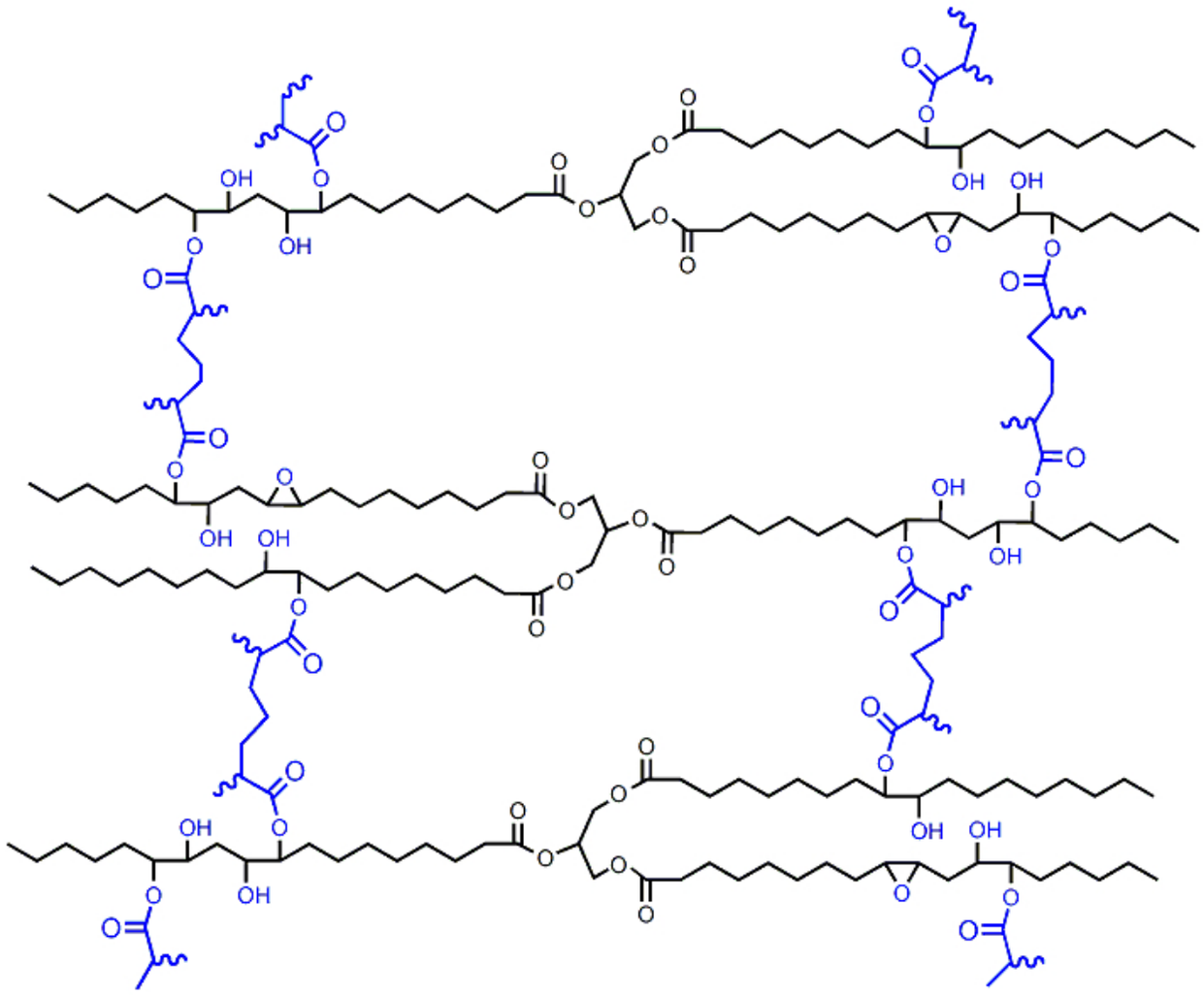

Figure 15. Representation of the 3D- polar paths (in blue) in which the CB particles surely disperse and preferentially distribute in all matrixes containing AESO comonomer.

4. Conclusions and remarks

It has been proved that polarity of the polymer matrix is very important in order to have a better distribution and dispersion of the conductive particles. However, AESO is a very interesting monomer that renders very low critical fractions under copolymerization with other polar comonomers as BMA and ACAB. The explanation we have is that AESO provides preferential distribution to the CB conductive particles due the 3D-crosslinking paths which are bonded to polar functional groups. This is the reason for thinking that conductive polymer composites based on AESO have a promising future in some applications as solvent, gases, vapors or pressure sensors. There are some previous results (unpublished) about the capacity for sensing solvents as well as pressure changes indicating they are very reliable and reproducible materials. The sensibility to pressure changes could be dependent on the crosslinking de-

gree, the proportion and on the comonomer chemical structure. Finally is considered that polymers derived from renewable sources could be a better alternative for reducing the oleopolymers use in some specific applications as discussed in this chapter.

Acknowledgements

Authors thank to the Universidad Autónoma del Estado de México under the projects 3135/2012FS and 3198/2012U for the financial support.

Author details

Susana Hernández López* and Enrique Vigueras Santiago*

*Address all correspondence to: eviguerass@uaemex.mx

Research and Development of Advanced Materials Laboratory, Chemistry Faculty of the State of Mexico Autonomous University, Toluca, Mexico

References

[1] Donnet, J. B., Bansal, R. C., & Wang, MJ. (1993). Carbon Black. *Science and Technology.*, USA: Marcel Dekker,.

[2] Kirkpatrick, S. (1973). Percolation and Conduction. *Reviews of Modern Physics*, 45(4), 574-578.

[3] Balberg, I. (1987). Tunneling and Nonuniversal Conductivity in Composite Materials. *Physical Review Letters*, 59(12), 1305-1308.

[4] Sisk, B. C., & Lewis, N. S. (2006). Vapor Sensing Using Polymer/Carbon Black Composites in the Percolative Conduction Regime. *Langmuir*, 22(18), 7928-7935.

[5] Yu, J., Zhang, L. Q., Rogunova, M., Summers, J., Hiltner, A., & Baer, E. (2005). Conductivity of Polyolefins Filled with High-Structure Carbon Black. *Journal of Applied Polymer Science*, 98(4), 1799-1805.

[6] Gaurav, R., Kasaliwal, Goldel. A., Potschke, P., & Heinrinch, G. (2011). Influences of Polymer Matrix Melt Viscosity and Molecular Weight on MWCNT agglomerate dispersion. *Polymer*, 52(4), 1027-1036.

[7] Cheng, G. S., Hu, J. W., Zhang, M. Q., Li, M. W., & Xiao, Rong. M. Z. (2004). Electrical Percolation of Carbon Black Filled Poly (ethylene oxide) Composites in Relation to the Matrix Morphology. *Chinese Chemical Letters*, 15(12), 1501-1504.

[8] Sumita, M., Abe, H., Kayati, M., & Miyasaka, K. (2006). Effect of Melt Viscosity and Surface Tension of Polymers on the Percolation Threshold of Conductive-Particle-Filled Polymeric Composites. *Journal of Macromolecules Science*, 25(1-2), 171 EOF-184 EOF.

[9] Tchoudakov, R., Breuer, O., & Narkis, Siegmann. A. (1996). Conductive Polymer Blends with Low Carbon Black Loading: Polypropylene/Polyamide. *Polymer Engineering and Science*, 36(10), 1336-1346.

[10] Sumita, M., Sakata, K., Asai, S., Miyasaka, K., & Nakagawa, H. (1991). Dispersion of Fillers and the Electrical Conductivity of Polymer Blends Filled with Carbon Black. *Polymer Bulletin*, 25(2), 265-271.

[11] Moriarty, G. P., Whittemore, J. H., Sun, K. A., Rawlins, J. W., & Grunlan, J. C. (2011). Influence of Polymer Particle Size on the Percolation Threshold of Electrically Conductive Latex-Based Composites. *Journal of Polymer Science*, Part B: Polymer Physics, 49(21), 1547-1554.

[12] Kasaliwal, G. R., Goldel, A., Potschke, P., & Heinrinch, G. (2011). Influences of Polymer Matrix Melt Viscosity and Molecular Weight on MWCNT Agglomerate Dispersion. *Polymer*, 52(4), 1027-1036.

[13] Cheng GS, Hu JW,. Zhang MQ, Li MW, Xiao DS, Rong MZ. (2004). Electrical Percolation of Carbon Black Filled Poly (Ethylene Oxide) Composites in Relation to the Matrix Morphology. *Chinese Chemical Letters*, 15(12), 1501-1504.

[14] Carmona, F. (1989). Conducting Filled Polymers. *Phisica A.*, 157(1), 461-469.

[15] Li, Y., Wang, S., Zhang, Y., & Zhang, Y. (2005). Electrical Properties and Morphology of Polypropylene/Epoxy/Glass Fiber Composites Filled with Carbon Black. *Journal of Applied Polymer Science*, 98(3), 1142-1149.

[16] Castro-Martínez, M., Hernández, López. S., & Vigueras, Santiago. E. (2012). Relationship Between Polymer-Chemical Structure and Electrical Properties in Conductive Carbon Black Composites. Submitted to e-Polymers.

[17] Hernández-López, S., Vigueras-Santiago, E., Mercado-Posadas, J., & Sánchez-Mendieta, V. (2006). Electrical Properties of Acrylated-Epoxidized Soybean Oil Polymers-Based Composites. *Advances in Technology of Materials and Materials Processing Journal*, 8(2), 214-219.

[18] Guner, F. S., Yagci, Y., & Erciyes, A. T. (2006). Polymer from Triglyceride Oils. *Progress in Polymer Science*, 31(7), 633-670.

[19] Sharma, V., & Kundu, P. P. (2006). Addition Polymers from Natural Oils- A Review. *Progress in Polymer Science*, 31(11), 983-1008.

[20] Meier, M. A. R., Metzger, J. O., & Shubert, U. S. (2007). Plant Oil Renewable Resources as Green Alternatives in Polymer Science. *Chemical Society Reviews*, 36(11), 1788-1802.

[21] Khot, S. N., Lascala, J. J., Can, E., Morye, S., Williams, G. I., Palmese, G. R., Kusefoglu, S. H., & Wool, R. P. (2001). Development and Application of Triglyceride-based Polymers and Composites. *Journal of Applied Polymer Science*, 82(3), 703-723.

[22] Blayo, A., Gandini, A., & Le Nest-F, J. (2001). Chemical and Rheological Characterizations of Some Vegetable Oils Derivates Commonly Used in Printing Inks. *Industrial Crops and Products*, 14(2), 155-167.

[23] Hill, K. (2000). Fats and Oils as Oleochemical Raw Materials. *Pure and Applied Chemistry*, 72(7), 1255-1264.

[24] Adhvaryu, A., & Erhan, S. Z. (2002). Epoxidized Soybean Oil as a Potential Source of High-Temperature Lubricants. *Industrial Crops and Products*, 15(3), 247-254.

[25] Tuman, S. J., Chamberlain, D., Scholsky, K. M., & Soucek, . (1996). Differential Scanning Calorimetry Study of Linseed Oil Cured with Metal Catalysts. *Progress in Organic Coatings*, 28(4), 251-258.

[26] Refvik, M. D., & Larock, R. C. (1999). The Chemistry of Metathesized Soybean Oil. *Journal of the American Oil Chemists´ Society*, 76(1), 99-102.

[27] Stemmelen, M., Pessel, F., Lapinte, V., Caillol, S., Habas-P, J., & Robin-J, J. (2011). A Fully Biobased Epoxy Resin from Vegetable Oils: From the Synthesis of the Precursors by Thiol-ene Reaction to the Study of the Final Material. *Journal of Polymer Science*, Part A: Polymer Chemistry, 49(11), 2434-2444.

[28] Erhan, S. Z., Bagby, M. O., & Nelsen, T. C. (1997). Drying Properties of Metathesized Soybean Oil. *Journal of the American Oil Chemists´ Society*, 74(6), 703-706.

[29] Montero de, Espinosa. L., & Meier, M. A. R. (2011). Plants Oils: The Perfect Renewable Resource for Polymer Science. *European Polymer Journal*, 47(5), 837-852.

[30] Teng, G., Wegner, J. R., Hurtt, G. J., & Soucek, MD. (2001). Novel Inorganic/Organic Hybrid Materials Based on Blown Soybean Oil with Sol-Gel Precursors. *Progress in Organic Coatings*, 42(1), 29-37.

[31] Andjelkovic, D. D., Vakverde, M., Henna, P., Li, F., & Larock, R. C. (2005). Novel Thermosets Prepared by Cationic Copolymerization of Various Vegetable Oils-Synthesis and Their Structure-Property Relationships. *Polymer*, 46(23), 9674-9685.

[32] Cakmakli, B., Hazer, B., Tekin, I. O., Kizgut, S., Koksal, M., & Menceloglu, Y. (2004). Synthesis and Characterization of Polymeric Linseed Oil Grafted Methyl Methacrylate or Styrene. *Macromolecular Bioscience*, 4(7), 649-655.

[33] Rybak, A., & Meier, M. A. R. (2008). Cross-Metathesis of Oleyl Alcohol with Methyl Acrylate: Optimization of Reaction Conditions and Comparison of Their Environmental Impact. *Green Chemistry*, 10(10), 1099-1104.

[34] Li, F., & Larock, R. C. (2000). Novel Polymeric Materials from Biological Oils. *Journal of Polymers and the Environment*, 59 EOF-67 EOF.

[35] Biermann, U., Friedt, W., Lang, S., Luhs, W., Machmuller, G., Metzger, J. O., Rusch, gen., Klaas, M., Schafer, H. J., & Schneider, M. P. (2000). *Angewandte Chemie International Edition*, 39(13), 2206-2224.

[36] Rusch, gen., Klaas, M., & Warwel, S. (1997). Lipase-Catalyzed Preparation of Peroxy Acids and Their Use for Epoxidation. *Journal of Molecular Catalysis: A Chemical*, 117(1-3), 311-319.

[37] La Scala, J., & Wool, R. P. (2002). Effect of FA Composition Kinetics of TAG. *Journal of the American Oil Chemists´ Society*, 9(4), 373-378.

[38] Okieimen FE, Bakare OI, Okieimen CO. (2002). Studies on the Epoxidation of Rubber Seed Oil. *Industrial Crops and Products*, 15(2), 139-144.

[39] Guidotti, M., Ravasio, N., Psaro, R., Gianotti, E., Coluccia, S., & Marchese, L. (2006). Epoxidation of Unsaturated FAMEs Obtained from Vegetable Source Over Ti(IV)-grafted Silica Catalysts: A Comparison between Ordered and Non-Ordered Mesoposous Materials. *Journal of Molecular Catalysis A: Chemical*, 250(1-2), 218-225.

[40] Campanella, A., Baltanas-Sánchez, Capel., Campos-Martín, M. C., Fierro, J. M., & , J. L. G. (2004). Soybean Oil Epoxidation with Hydroperoxide Using an Amorphous Ti/Si Catalysts. Green Chemistry , 6(7), 330-334.

[41] Parreira, T. F., Ferreira, M. M. C., Sales, H. J. S., & de Almeida, W. B. (2002). Quantitative Determination of Epoxidized Soybean Oil using Near-Infrared Spectroscopy and Multivariate Calibration. *Applied Spectroscopy*, 56(12), 1607-1614.

[42] Vlcek, T., & Petrovic, Z. S. (2006). Optimization of the Chemoenzymatic Epoxidation of Soybean Oil. *Journal of the American Oil Chemists´ Society*, 83(3), 247-252.

[43] Hilker, I., Bothe, D., Pruss, J., & Warnecke-J, H. (2001). Chemo-Enzimatic Epoxidation of Unsatured Plant Oils. *Chemical Engineering Science*, 56(2), 427-432.

[44] Rusch, gen., Klaas, M., & Warwel, S. (1999). Complete and Partial Epoxidation of Plant Oils by Lipase-Catalyzed Perhydrolysis. *Industrial Crops and Products*, 9(2), 125-132.

[45] López-Téllez, G., Vigueras-Santiago, E., & Hernández-López, S. (2009). Characterization of Linseed Oil Epoxidized at Different Percentages. *Superficies y Vacío*, 22(1), 5-10.

[46] Muturi, P., Wang, D., & Dirlikov, S. (1994). Epoxidized Vegetable Oils as Reactive Diluents I. Comparison of Vernonia, Epoxidized Soybean and Epoxidized Linseed Oils. *Progress in Organic Coatings*, 25(1), 85-94.

[47] Tan, S. G., & Chow, W. S. (2010). Biobased Epoxidized Vegetable Oils and Its Greener Epoxy Blends: A Review. *Polymer-Plastics Technology and Engineering*, 49(15), 1581-1590.

[48] Jin F-L, Park S-J. (2007). Thermal and Rheological Properties of Vegetable Oil-Based Epoxy Resins Cured with Thermally Latent Initiator. *Journal of Industrial Engineering of Chemistry*, 13(5), 808-814.

[49] Uyama, H., Kuwabara, M., Tsujimoto, T., Nakano, M., Usuki, A., & Kobayashi, S. (2003). Green Nanocomposites from Renewable Resources: Plant Oil-Clay Hybrid Materials. *Chemistry of Materials*, 15(13), 2492-2494.

[50] Samuelsson, J., Sundell-E, P., & Johansson, M. (2004). Synthesis and Polymerization of a Radiation Curable Hyperbranched Resin Based on Epoxy Functional Fatty Acids. *Progress in Organic Coatings*, 50(3), 193-198.

[51] Chakrapani, S., & Crivello, J. V. (1998). Synthesis and Photoinitiated Cationic Polymerization of Epoxidized Castor Oil and Its Derivates. *Pure and Applied Chemistry A*, 35(1), 1-20.

[52] Crivello, J. V. (2008). Effect of Temperature on the Cationic Photopolymerization of Epoxides. *Journal of Macromolecular Science, Part A: Pure and Applied Chemistry*, 45(8), 591-598.

[53] Cheong, M. Y., Ooi, T. L., Amhad, S., Wan, M. Z. W. Y., & Kuang, D. (2009). Synthesis and Characterization of Palm-Based Resin for UV Coating. *Journal of Applied Polymer Science*, 111(5), 2353-2361.

[54] López-Téllez, G., Vigueras-Santiago, E., & Hernández, López. S. (2008). Synthesis and Thermal Cross-Linking Study of Partially-Aminated Epoxidized Linseed Oil. *Designed Monomers and Polymers*, 11(5), 435-445.

[55] Manthey, N. W., Cardona, F., Aravinthan, T., & Cooney, T. (2011). Cure Kinetics of an EpoxidIzed Hemp Oil based Bioresin System. *Journal of Applied Polymer Science*, 122(1), 444-451.

[56] Rosch, J., & Mulhaupt, R. (1993). Polymers from Renewable Resources: Polyester Resins and Blends upon Anhydride-Cures Epoxidized Soybean Oil. *Polymer Bulletin*, 31(6), 679-665.

[57] Gerbase, A. E., Petzhold, C. L., & Costa, A. P. O. (2002). Dynamical Mechanical and Thermal Behavior of Epoxy Resins Based on Soybean Oil. *Journal of the American Oil Chemists´ Society*, 79(8), 797-802.

[58] Yue, S., Hu, J. F., Huang, H., Fu, H. Q., Zeng, H. W., & Chen, H. Q. (2007). Synthesis, Properties and Application of Novel Epoxidized Soybean Oil Toughened Phenolic Resins. *Chinese Journal of Chemical Engineering*, 15(3), 418-423.

[59] Munoz, J. C., Ku, H., Cardona, F., & Rogers, D. (2008). Effects of Catalysts and Post-Curing Conditions in the Polymer Network of Epoxy and Phenolic Resins: Preliminary results. *Journal of Materials Processing Technology*, 486 EOF-492 EOF.

[60] Kiatsimkul, P-p., Suppes, G. J., Hsieh, F-h., Lozada, Z., & Tu-C, Y. (2008). Preparation of High Hydroxyl Equivalent Weight Polyols from Vegetable Oils. *Industrial Crops and Products*, 27(3), 257-264.

[61] Hofer, R., Daute, P., Grutzmacher, R. K., & Ga-H, A. A. W. (1997). Oleochemical Polyols-A New Raw Material Source for Polyurethane Coatings and Floorings. *Journal of Coatings Technology*, 69(869), 65-72.

[62] Zlatanić, A., Lava, C., Zhang, W., & Petrović, Z. S. (2004). Effect of Structure on Properties of Polyols and Polyurethanes Based on Different Vegetable Oils. *Journal of Polymer Science Part B: Polymer Physics*, 42(5), 809-819.

[63] Lligadas, G., Ronda, J. C., Galià, M., & Cádiz, V. (2010). Plant Oils as Platform Chemicals for Polyurethane Synthesis: Current State-of-the-Art. *Biomacromolecules*, 11(11), 2825-2835.

[64] La Scala, J., & Wool, R. P. (2002). The Effect of Fatty Acid Composition on the Acrylation Kinetics of Epoxidized Triacylglycerols. *Journal of the American Oil Chemistis´ Society*, 79(1), 59-6.

[65] Li, F., Hanson, M. V., & Larock, R. C. (2001). Soybean Oil-Styrene-Divinylbenzene Thermosetting Polymers: Synthesis, Structure, Properties and Their Relationships. *Polymer*, 42(4), 1567-1579.

[66] Li, F., & Larock, R. C. (2002). New Soybean Oil-Styrene-Divinylbenzene Thermosetting Copolymers V: Shape-Memory Effect. *Journal of Applied Polymer Science*, 84(8), 1533-1543.

[67] Li, F., & Larock, R. C. (2002). Novel Polymeric Materials from Biological Oils. *Journal of Polymers and the Environment*, 59 EOF-67 EOF.

[68] Zhang, M., Wool, R. P., & Xiao, J. Q. (2001). Electrical Properties of Chicken Feather Fiber Reinforced Epoxy Composites. *Composites Part A: Applied Science and Manufacturing*, 42(3), 229-233.

[69] Teng, G., & Soucek, . (2000). Epoxidized Soybean Oil-Based Ceramer Coatings. *Journal of the American Oil Chemists´ Society*, 77(4), 381-387.

[70] La Scala, J., & Wool, R. P. (2005). Property Analysis of Triglyceride-Based Thermosets. *Polymer*, 46(1), 61-69.

[71] Vigueras-Santiago, E., Hernández-López, S., Linares-Hernández, K., & Linares-Hernández, I. (2009). Mechanical Properties of Goat Leather Photo Grafted with Acrylate-Epoxidized Linseed Oil. *Advances in Technology of Materials and Materials Processing Journal*, 11(2), 43-48.

[72] Ureña-Núñez, F., Vigueras-Santiago, E., Hernández-López, S., Linares-Hernández, K., & Linares-Hernández, I. (2008). Structural, Thermal and Morphological Characterization of UV-Graft Polymerization of Acrylated-Epoxidized Soybean Oil onto Goat Leather. *Chemistry and Chemical Technology*, 2(3), 191-197.

[73] Hernández-López, S., Martín-López del, Campo., Sánchez-Mendieta, E., Ureña-Núñez, V., Vigueras, F., & Santiago, E. (2006). Gamma Irradiation Effect on Acrylated-Epoxi-

dized Soybean Oil: Polymerization and Characterization. *Advances in Technology of Materials and Materials Processing Journal*, 8(2), 220-225.

[74] Williams, G. I., & Wool, R. P. (2000). Composites from Natural Fibers and Soy Oil Resins. *Applied Composites Materials*, 7(5-6), 421 EOF-432 EOF.

[75] Oprea, S. (2010). Properties of Polymer Networks Prepared by Blending Polyester Urethane Acrylate with Acrilated Epoxidized Soybean oil. *Journal of Materials Science*, 45(5), 1315-1320.

[76] Thielemans, W., & Wool, R. P. (2004). Butyrated Kraft Lignin as Compatibilizing Agent for Natural Fiber Reinforced Thermoset Composites. *Composites Part A Applied Sciencie and Manufacturing*, 35(3), 327-338.

[77] Dweib, Hu. B., O´, Donnell. A., Shenton, H. H., & Wool, R. P. (2004). All Natural Composite Sandwich Beams for Structural Applications. *Composite Structures*, 63(2), 147-157.

[78] Dweib, Hu. B., Shentin, I. I. I. H. W., & Wool, R. P. (2006). Bio-Based Composite Roof Structures: Manufacturing and Processing Issues. *Composite Structures*, 74(4), 379-388.

[79] Panhuis, M., in, H., Thielemans, W., Minett, A. I., Leahy, R., Le Foulgoc, B., Blau, W. J., & Wool, R. P. (2003). A Composite from Soy Oil and Carbon Nanotubes. *International Journal of Nanoscience*, 2(3), 185-194.

[80] Thielemans, W., Mc Aninch, I. M., Barron, V., Blau, W. J., & Wool, R. P. (2005). Impure Carbon Nanotubes as Reinforcements for Acrylated Epoxidized Soy Oil Composites. *Journal of Applied Polymer Science*, 98(3), 1325-1338.

[81] San-Farfán, Juan., Hernández-López, R., Martínez-Barrera, S., Camacho-López, G., Vigueras-Santiago, M. A., & , E. (2005). Electrical Characterization of Polystyrene-Carbon Black Composites. *Physica Status Solidi*, 2-3762.

[82] Verbanac, F. (1985). Cellulosic Organic Solvent Soluble Products. Patent USA,(4)

[83] Edgar, K. J., Buchanan, CM, Debenham, JS, Rundquist, PA, Seiler, BD, Shelton, MC, & Tindall, D. (2001). Advances in cellulose ester performance and application. *Progress in Polymer Science*, 26(9), 1605-1688.

[84] Verbanac, F. (1984). Cellulosic Organic Solvent Soluble Products. Patent number 4,490,516, Dec 25,.

[85] Shediac, R., Ngola, S. M., Throckmorton, D. J., Anex, Shepodd. T. J., & Singh, A. K. (2001). Reversed-Phase Electrochromatography of Amino Acids and Peptides Using Porous Polymer Monoliths. *Journal of Chromatography*, 925(1-2), 251 EOF-63 EOF.

[86] Carbon Black User´s Guide, (2006). International Carbon Black Association,. ., 28.

[87] Columbian Chemicals Company. (2010). http://www.columbianchemicals.com/Portals/Markets%20and%20Applications/Industrial%20Carbon%20Black/Inks/CCC_lores_Raven_0505.pdf, (accessed 1 August).

[88] Cabot Corporation:. (2010). http://www.cabot-corp.com/wcm/download/en-us/sb/VULCAN_XC72-English1.pdf, (accessed 1 August).

[89] Nhumo^{MR} . (2010). http://www.nhumo.com.mx/UploadedFiles/Adjunto-Standard_Carbon_Blacks-200671910496.pdf, (accessed 1 August).

[90] Brostow, W., Keselman, M., Mironi-Harpz, I., Narkis, M., & Peirce, R. (2005). Effects of Carbon Black on Tribology of Blends of Poly(Vinylidene Fluoride) with Irradiated an Non-Irradiated Ultrahigh Molecular Weight Polyethylene. *Polymer*, 46(14), 5058-5064.

[91] Marinho, B., Ghislandi, M., Tkalya, E., Koning, CE, & de With, G. (2012). Electrical Conductivity of Compacts of Graphene, Multiwalled Carbon Nanotubes, Carbon Black, and Graphite Powder. *Powder Technology*, 221(1), 351-358.

[92] Celzard, A., Marêché, J. F., Payot, F., & Furdin, G. (2002). Electrical Conductivity of Carbonaceous Powders. *Carbon*, 40(15), 2801-2815.

[93] Vigueras, Santiago. E., Hernández, López. S., & Mercado, Posadas. J. (2009). Modificación de propiedades eléctricas en compuestos poliméricos con negro de carbono. In: Camacho-López M.A, et al (ed), *Tópicos en Materiales,*, México: Universidad Autónoma del Estado de México;.

IntechOpen